Inorganic Chemistry

Article

pubs.acs.org/IC

Highly Selective and Sensitive Luminescence Turn-On-Based Sensing of Al^{3+} Ions in Aqueous Medium Using a MOF with Free Functional Sites

Debal Kanti Singha and Partha Mahata*

Department of Condensed Matter Physics and Material Sciences, S. N. Bose National Centre for Basic Sciences, Block-JD, Sec-III, Salt Lake City, Kolkata 700098, India

Supporting Information

ABSTRACT: A new metal−organic framework [Co(OBA)-$(DATZ)_{0.5}(H_2O)$] {OBA = 4,4′-oxybis(benzoic acid) and DATZ = 3,5-diamino-1,2,4-triazole}, **1**, was synthesized by hydrothermal reaction. Single-crystal X-ray data of **1** confirmed two-dimensional rhombus grid network topology with a free nitrogen site of triazole ring and two amine groups of each DATZ. Photoluminescence study of **1** in aqueous medium shows blue emission at 407 nm upon excitation at 283 nm. This emissive property was used for the sensing of Al^{3+} ions in aqueous medium through very high luminescence turn-on (6.3-fold) along with the blue shifting (~24 nm) of the emission peak. However, luminescence studies in the presence of other common metal ions such as Mg^{2+}, Zn^{2+}, Ni^{2+}, Co^{2+}, Mn^{2+}, K^+, Na^+, Ca^{2+}, Cd^{2+}, Hg^{2+}, Cu^{2+}, Fe^{2+}, Fe^{3+}, and Cr^{3+} in aqueous medium shows luminescence quenching in varying extent. Interestingly, the luminescence turn-on-based selectivity of Al^{3+} ions in aqueous medium was achieved even in the presence of the highest quenchable metal ion, Fe^{3+}. Furthermore, very high sensitivity was observed in the case of Al^{3+} ions with a limit of detection of Al^{3+} of 57.5 ppb, which is significantly lower than the higher limit of U.S. Environmental Protection Agency recommendation of Al^{3+} ion for drinking water (200 ppb).

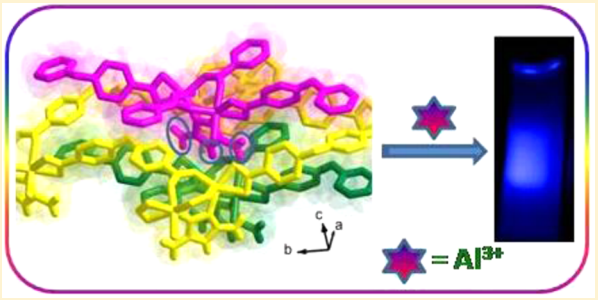

INTRODUCTION

Aluminum is one of the widely used metals in industry.[1] The trivalent cation of aluminum (Al^{3+}) existing in natural water and most plants can enter the human body through foods and drinking water.[2] The average daily uptake of Al^{3+} ions for the human body is about 3−10 mg/day.[3] However, aluminum is not a trace element necessary for human body, and its presence in high concentration in the human body has adverse effect on human health, for instance, Parkinson's disease.[4] Because of the everyday use of aluminum foil and containers, the risk of absorption of Al^{3+} ions by the human body is increasing. Additionally, the iron binding protein can carry Al^{3+} ions to the brain to damage the central nervous system.[5] More importantly, the presence of excess amount in human brain can also lead to Alzheimers's disease.[6] Thus, the detection of Al^{3+} has attracted increasing interest in the areas of environmental and medical sciences.

Among the sensing methods, luminescence-based methods have gained much attention in recent years due to their advantageous features such as ease of manipulation, high sensitivity, and real-time monitoring with rapid response time.[7] Recently, some luminescent sensors with detection of Al^{3+} ions have been reported,[8] and even fewer sensors have been reported for sensing in pure water.[4b,9] Nevertheless, their widespread use is limited owing to multistep processing, requirement of expensive chemicals, stability, and lack of molecular organization.[2a] Therefore, it is important to develop a simple sensor with high selectivity and sensitivity for Al^{3+} in aqueous medium.

Metal−organic frameworks (MOFs) are relatively a new class of hybrid crystalline materials with diverse structural characteristics and tunable pore size constructed by the connectivity of metal ions or metal clusters and organic ligands.[10] MOFs have shown a variety of potential applications such as gas storage,[11] gas separation,[12] catalysis,[13] magnetism,[14] drug delivery,[15] bioimaging,[16] and proton conductivity.[17] Recently, significant progress has been made in the uses of the luminescence property of MOFs for sensing of small molecules,[18] metal ions,[19] and explosives.[20] Generally the diverse pore topologies and functional sites make MOFs as suitable sensory materials through the molecular level interactions between the framework and the analytes.[19g] An efficient strategy to prepare MOFs for the use of metal ion sensing is to use aromatic organic molecules with nonbonded functional ligand sites, in which the aromatic part provides luminescence, and the nonbonded functional sites interact with the metal ions.[21] However, immobilization of functional site within the MOFs has been still challenging due to their high reactivity during the synthesis of MOFs.[19n]

Recently two Eu-based luminescent MOFs have been used for the sensing of Al^{3+} ions in dimethylformamide solvent,[19h,l]

Received: March 27, 2015
Published: June 8, 2015

DOI: 10.1021/acs.inorgchem.5b00688
Inorg. Chem. 2015, 54, 6373−6379

but there are no reports of sensing of Al^{3+} ions using MOF in aqueous medium. On the basis of the above consideration, we synthesized a new two-dimensional MOF $[Co(OBA)(DATZ)_{0.5}(H_2O)]$ {OBA = 4,4′-oxybis(benzoic acid) and DATZ = 3,5-diamino-1,2,4-triazole}, **1**, with rhombus grid network topology with free nitrogen site of triazole ring and amine groups of DATZ employing hydrothermal reaction. On the exposure of UV light **1** shows visible blue emission. It senses Al^{3+} ions through 6.3-fold luminescence turn-on and blue shifting of the emission peak position in aqueous medium. The compound shows luminescence quenching in varying extent in aqueous medium in the presence of other common metal ions such as Mg^{2+}, Zn^{2+}, Ni^{2+}, Co^{2+}, Mn^{2+}, K^{+}, Na^{+}, Ca^{2+}, Cd^{2+}, Hg^{2+}, Cu^{2+}, Fe^{2+}, Fe^{3+}, and Cr^{3+}. The selectivity of Al^{3+} ion detection was achieved even in the presence of the highest quenchable metal ion, Fe^{3+}. The very high sensitivity and completely different luminescence behavior in the presence of Al^{3+} ions is clear indication of strong preferential molecular level interaction between the MOF and Al^{3+} ion. This is first observation, to our knowledge, where an MOF is used for the selective sensing of Al^{3+} ions in aqueous medium. In this paper, we present the synthesis, characterization, and sensing behavior of **1**.

EXPERIMENTAL SECTION

Materials. The chemicals required for the synthesis of **1**, $Co(NO_3)_2·6H_2O$ (Merck, 98%), 4,4′-oxybis(benzoic acid) (Sigma-Aldrich, 99%), 3,5-diamino-1,2,4-triazole (Sigma-Aldrich, 98%), and NaOH (Merck, 97%) were used as received. The chemicals used for the detection experiments, anhydrous $AlCl_3$ (Merck, 98%), anhydrous $FeCl_3$ (Merck, 98%), $Cr(NO_3)_3·9H_2O$ (Sigma-Aldrich, 99%), $FeCl_2·4H_2O$ (Sigma-Aldrich, 99%), $CuCl_2·2H_2O$ (Merck, 98.5%), $HgCl_2$ (Merck, 99.5%), $CdCl_2·H_2O$ (Merck, 98%), $CaCl_2$ (Merck, 98%), NaCl (Merck, 99%), KCl (Merck, 98.5%), $MnCl_2·4H_2O$ (Merck, 99%), $CoCl_2·6H_2O$ (Merck, 98%), $NiCl_2·6H_2O$ (Sigma-Aldrich, 98%), $ZnSO_4·7H_2O$ (Merck, 99%), and $MgCl_2·6H_2O$ (Merck, 98%), were used as received without further purification. The water used was doubly distilled and filtered through a Millipore membrane.

Synthesis. The title compound was prepared employing the hydrothermal method. $Co(NO_3)_2·6H_2O$ (0.2910 g, 1 mM) and 4,4′-oxybis(benzoic acid) (0.2608 g, 1 mM) were dispersed in 10 mL of water. 3,5-Diamino-1,2,4-triazole (0.101 g, 1 mM) and NaOH (0.08 g, 2 mM) were added with continuous stirring, and the mixture was homogenized at room temperature for 30 min. The final reaction mixture was sealed in a 23 mL polytetrafluoroethylene-lined stainless steel autoclave and heated at 180 °C for 72 h. The initial pH value of the reaction mixture was 5, and no appreciable change in pH was noted after the reaction. The final product, containing large quantities of dark pink-colored plate-shaped rectangular crystals, was filtered, washed with deionized water under vacuum, and dried at ambient conditions (yield 70% based on Co). Anal. Calcd (%) for **1**: C 47.03, H 3.27, N 9.15; found: C 46.9, H 3.24, N 9.21.

Initial Characterizations. Powder X-ray diffraction (XRD) patterns were recorded on well-ground samples in the 2θ range of 5−50° using Cu Kα radiation (Rigaku Miniflex diffractometer; see Supporting Information, Figure S1). The XRD patterns indicated that the product is a new material; the pattern is entirely consistent with the simulated XRD pattern generated based on the structure determined using the single-crystal XRD. The IR spectrum was recorded on a KBr pellet (JASCO FT/IR-6300; see Supporting Information, Figure S2). The observed IR frequencies are listed in Table S1 (see Supporting Information). Thermogravimetric analysis (TGA) using PerkinElmer Diamond instrument was performed in nitrogen atmosphere (flow rate = 20 mL min^{-1}) in the temperature range of 30−800 °C (heating rate = 10 °C min^{-1}; see Supporting Information, Figure S3). The TGA studies shows weight loss in two distinct steps. The first weight loss of 4.8% up to 145 °C may be due to the removal of the coordinated water molecules, and the second weight loss in the range of 350−610 °C leads to the decomposition of the framework. The total observed weight loss of 85% corresponds well with the loss of water molecules, DATZ, and OBA ligands (calcd 85.1%). The differential scanning calorimetric (DSC) measurement was also performed using TA Instrument Q2000 at a heating rate of 10 °C min^{-1} from 30 to 350 °C under nitrogen atmosphere (see Supporting Information, Figure S4). The DSC plot shows endothermic peaks in range of 75−180 °C, which corresponds to the removal of coordinated water. The total molar enthalpy of dehydration calculated from the DSC measurements is 6.0 kcal. The morphologies of **1** were investigated using scanning electron microscope (QUANTA FEG250, FEI). Magnetic susceptibility measurements were performed on a superconducting quantum interference device (SQUID) magnetometer.

Single-Crystal Structure Determination. A suitable single crystal was carefully selected under a polarizing microscope and glued carefully to a thin glass fiber. The single-crystal data were collected on a Bruker AXS smart Apex CCD diffractometer at 293(2) K. The X-ray generator was operated at 50 kV and 35 mA using Mo Kα (λ = 0.710 73 Å) radiation. Data were collected with ω scan width of 0.3°. A total of 606 frames were collected in three different settings of φ (0, 90, 180°) keeping sample-to-detector distance fixed at 6.03 cm and the detector position (2θ) fixed at −25°. The data were reduced using SAINTPLUS,[22] and an empirical absorption correction was applied using the SADABS program.[23] The structure was solved and refined using SHELXL97[24] present in the WinGx suit of programs (Version 1.63.04).[25] All the hydrogen atoms were initially located in the difference Fourier maps, and for the final refinement, the hydrogen atoms were placed in geometrically ideal positions and held in the riding mode. Final refinement included atomic positions for all the atoms, anisotropic thermal parameters for all the non-hydrogen atoms, and isotropic thermal parameters for all the hydrogen atoms. Full-matrix least-squares refinement against $|F^2|$ was performed using the WinGx package of programs.[25] Details of the structure solution and final refinement is given in Table 1. Additional crystallographic information is available in the Supporting Information.

Table 1. Crystal Data and Structure Refinement Parameters for $[Co(C_{14}H_8O_5)(C_2N_5H_5)_{0.5}(H_2O)]$, 1

empirical formula	$C_{15}H_{12.5}O_6N_{2.5}Co$
formula weight	382.71
crystal system	orthorhombic
space group	*Aba*2 (No. 41)
a (Å)	14.0280(4)
b (Å)	29.3136(8)
c (Å)	7.3395(2)
volume (Å^3)	3018.08(14)
Z	8
T (K)	296(2)
ρ_{calc} (g cm^{-3})	1.685
μ (mm^{-1})	1.175
θ range (deg)	1.39 to 27.99
λ (Mo Kα) (Å)	0.710 73
R indices[a] [$I > 2\sigma(I)$]	R_1 = 0.0319, wR_2 = 0.0798
R indices[a] (all data)	R_1 = 0.0372, wR_2 = 0.0948

[a] $R_1 = \sum||F_0| - |F_c||/\sum|F_0|$; $wR_2 = \{\sum[w(F_0^2 - F_c^2)^2]/\sum[w(F_0^2)^2]\}^{1/2}$. $w = 1/[\sigma^2(F_0)^2 + (aP)^2 + bP]$, $P = [\max(F_0^2,0) + 2(F_c)^2]/3$, where a = 0.0620 and b = 0.1426

Optical Measurement. Photoluminescence properties of **1** dispersed in water were investigated at room temperature using a Fluorolog Horiba Jobin-Yvon spectrofluorometer. The dispersed solutions were prepared by mixing 1.913 mg of **1** into 100 mL of water in a volumetric flask followed by ultrasonic agitation for 10 min. The photoluminescence measurements were performed using 2 mL of the dispersion in quartz cuvette.

DOI: 10.1021/acs.inorgchem.5b00688
Inorg. Chem. 2015, 54, 6373−6379

RESULTS AND DISCUSSION

Structure and Morphology. The asymmetric unit of **1** consists of one crystallographically independent Co^{2+} ion, one OBA, half DATZ, and one coordinated water molecule (see Supporting Information, Figure S5). The Co^{2+} ion is octahedrally (distorted) coordinated by four carboxylate oxygen atoms, one nitrogen atom of the triazole ring, and one water molecule (see Supporting Information, Figure S6a). Of the two carboxylate groups of the OBA, one is bidentate with two different Co^{2+} ions, and the other one is bidentate with the same Co^{2+} ion (see Supporting Information, Figure S6b); the DATZ connects two Co^{2+} ions through nitrogen atoms of 1 and 2 positions of the triazole ring. The two amino groups (at 3 and 5 postions) of the triazole ring remain uncoordinated (see Supporting Information, Figure S6c). The Co−O bonds have average distances of 2.12 Å, and the Co−N bond has distance of 2.05 Å. The O/N−Co−O/N bond angles are in the range of 60.28 (8)−172.22 (9)°. The selected bond distances are listed in Table 2, and the selected bond angles are listed in Table S2 (see Supporting Information).

Table 2. Selected Bond Distances (Å) Observed in $[Co(C_{14}H_8O_5)(C_2N_5H_5)_{0.5}(H_2O)]$, 1

bond	distances, Å	bond	distances, Å
Co(1)−N(1)	2.053(2)	Co(1)−O(6)	2.103(2)
Co(1)−O(2)[a]	2.064(2)	Co(1)−O(4)	2.176(2)
Co(1)−O(1)	2.0765(19)	Co(1)−O(3)	2.184(2)

[a]Symmetry operations used to generate equivalent atoms: $-x + 2, -y, z$.

The structure contains a Co_2 dimeric unit of the formula $[Co_2(C_2N_3H_5)(COO)_4(H_2O)_2]$, formed by the connectivity of two cobalt ions through carboxylate groups of OBA and nitrogen atoms of DATZ (Figure 1a). The dimers are connected by the OBA ligands to form a two-dimensional rhombus grid network topology (Figure 1b). The rhombus grid layers are arranged in an ABAB... fashion, giving rise to rectangular-shaped micropores (see Supporting Information, Figure S7a). One nonbonded nitrogen atom (NH) of triazole ring and two nonbonded amino groups of the DATZ are oriented toward the pores formed by the packing of A and B layers (see Supporting Information, Figure S7b). These free functional sites of DATZ have significant role for the selective sensing of Al^{3+} ions in aqueous medium.

The powder sample of **1** was analyzed using scanning electron microscopy (SEM) by drop casting in silicon wafer to evaluate the morphologies. The powder grains are plate shaped with various sizes in micron region (see Supporting Information, Figure S8).

Magnetic Studies. Temperature-dependent magnetic susceptibility measurements on powder samples were performed using a SQUID magnetometer (see Supporting Information, Figure S9a). In the case of octahedrally coordinated Co^{2+} compounds, the first-order spin orbital interactions and the orbital contribution have significant role in magnetic moment due to the orbitally degenerate electronic ground state. In present compound the orbital contribution has significant input in the magnetic moment at room temperature. The effective magnetic moment of compound **1** at room temperature (300 K) is 4.8 μ_B, which corresponds to the value expected for octahedral Co^{2+} ions with significant orbital contribution as the spin-only moment is 3.87 μ_B. A plot of $1/\chi_M$ versus T is linear from 50 to 300 K with a Weiss temperature of −10.5 K and a Curie constant of 2.97 emu/mol. The negative Weiss temperature observed for **1** results from the presence of a weak antiferromagnetic interaction in **1**. The nature of $\chi_M T$ versus T and M versus H at 2.1 K also supports the antiferromagnetic behavior (see Supporting Information, Figure S9b,c).

Metal-Ion Detections. The compound **1** when dispersed in water exhibited blue emission centered at 407 nm upon excitation at 283 nm (Figure 2). The emission observed is due to intraligand transitions ($\pi^* \rightarrow \pi$ and $\pi^* \rightarrow$ n transitions) of two aromatic ligands bonded with the metal ions. To explore the ability of **1** to sense a trace amount of metal ions, luminescence-based titrations were performed with the incremental addition of analytes (metal ions) to **1** dispersed in water. Figure 3 shows changes in the luminescence intensity with the increasing addition of Al^{3+} ions (up to 50 μM). The blue emission of **1** on UV exposure is intensified upon the addition of Al^{3+} ions (Figure 3 inset), which is nearly 6.3 times of the initial luminescence intensity along with the blue shifting of ∼24 nm of the emission peak. Similar luminescence-based titrations were also performed with other metal ions such as Mg^{2+}, Zn^{2+}, Ni^{2+}, Co^{2+}, Mn^{2+}, K^+, Na^+, Ca^{2+}, Cd^{2+}, Hg^{2+}, Cu^{2+}, Fe^{2+}, Fe^{3+}, and Cr^{3+} (see Supporting Information, Figure S10−S23). Significant luminescence quenching was observed in the case of Fe^{3+}, Cr^{3+}, and Fe^{2+} ions. The changes of luminescence intensity based on the emission at 407 nm in the case of all metal ions after the addition of 50 μM metal ions shown in Figure 4 as bar diagram with respect of $[(I/I_0) - 1]$ (I = luminescence intensity after the addition of 50 μM metal ions, I_0 = luminescence intensity before the addition of metal ions) values. These results indicate luminescence behavior of **1** can be significantly different only in the presence of Al^{3+} ions. The luminescence turn-on behavior in the presence of Al^{3+} ions in aqueous medium can be clearly detected at as low as 2.5 μM concentration, which is equivalent to 57.5 ppb of Al^{3+} ions in water (see Supporting Information, Figure S24). The observed detection limit is significantly lower than the higher limit of U.S. Environmental Protection Agency (EPA) recommendation of Al^{3+} ion for drinking water (200 ppb).[26]

Motivated by very high luminescence turn-on in the presence of Al^{3+} ions, we thought to check the selectivity for Al^{3+} ions in the presence of Fe^{3+} ions (the highest quenchable metal ions). In a specially designed experimental protocol, the luminescence spectrum of **1** in aqueous medium was recorded, and to this 2 μL of 0.01 M aqueous solution of Fe^{3+} ions was added sequentially in two equal portions (1 μL in each portion) followed by 2 μL of 0.01 M aqueous solution of Al^{3+} ions in similar way; the corresponding emissions were monitored. The Fe^{3+} ions were added initially, but the addition of Fe^{3+} ions showed small luminescence quenching. However, the addition of aqueous solution of Al^{3+} ions gave significant luminescence turn-on, with the turn-on efficiency of Al^{3+} remaining unaffected, even through further addition sequences (see Supporting Information, Figure S25). The results can be easily visualized by plotting the percentage of luminescence intensity versus volume of analyte added (Figure 5). The stepwise overall increase in luminescence intensity clearly demonstrates high selectivity of the **1** for Al^{3+} ions in the presence of Fe^{3+} ions.

The very high luminescence intensity of **1** in the presence of Al^{3+} ions was compared with the well-known luminescent material tris(8-hydroxyquinoline)aluminum (AlQ_3). The lumi-

DOI: 10.1021/acs.inorgchem.5b00688
Inorg. Chem. 2015, 54, 6373−6379

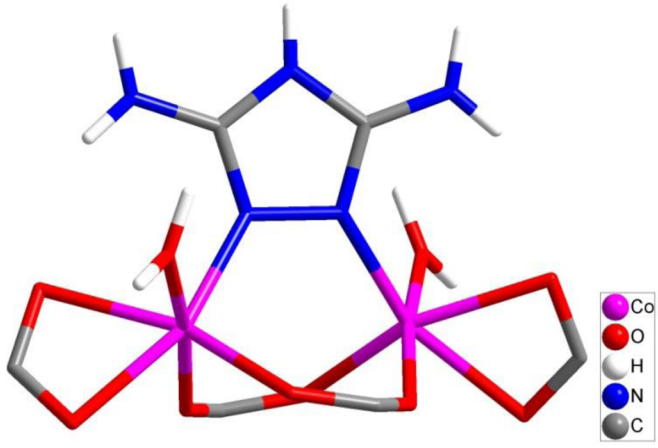

(a)

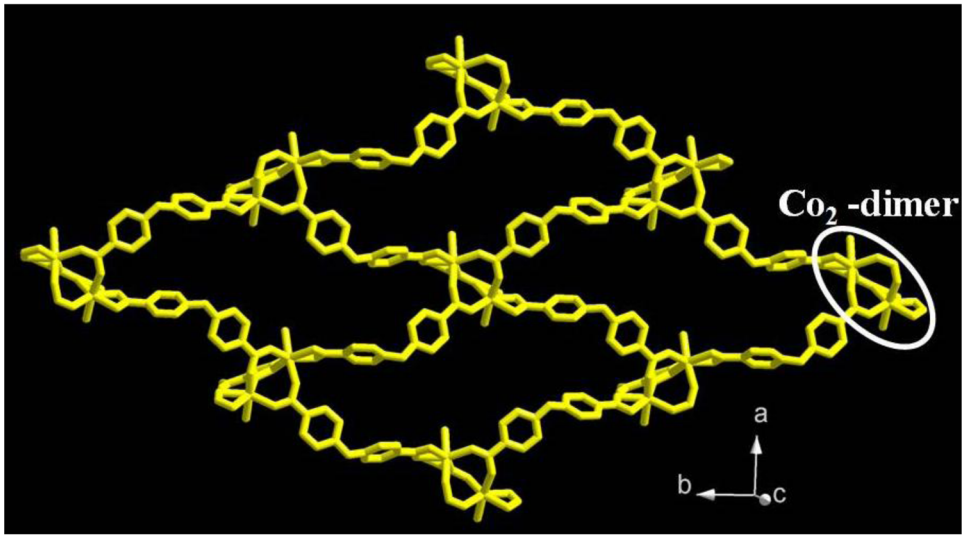

(b)

Figure 1. (a) The structure of Co_2 dimeric unit of the formula $[Co_2(C_2N_3H_5)(COO)_4(H_2O)_2]$, formed by the connectivity of two cobalt ions through carboxylate groups of OBA and nitrogen atoms of DATZ in $[Co(C_{14}H_8O_5)(C_2N_5H_5)_{0.5}(H_2O)]$, **1**. (b) Two-dimensional rhombus grid network formed from the connectivity between Co_2 dimeric units and OBA ligands.

nescence properties of the composite solution of Al^{3+} ions and MOF (based on one Al^{3+} ion per triazole unit) and the AlQ_3 were studied in aqueous medium. For this the two solutions (Al^{3+}@MOF and AlQ_3) with identical molar strength were prepared. This study indicates Al^{3+}@MOF composite and AlQ_3 show blue (centered at 397 nm, λ_{ex} = 283 nm) and bluish-green emissions (centered at 495 nm, λ_{ex} = 283 nm), respectively, with comparable luminescence intensity (see Supporting Information, Figure S26).

To check the recyclability for the Al^{3+} sensing, luminescence experiments were performed using 3.3 mg of **1** dispersed in 2 mL of water in a quartz cuvette, and the emission data were recorded (see Supporting Information, Figure S27). After Al^{3+} ions with 30 μM concentration were added, the emission data show 2.21 times increase in intensity with the blue shifting (~20 nm). The solid compound was collected from the solution through centrifugation and washed with water several times. The similar luminescence experiment using the collected solid (**1**) showed comparable luminescence intensity at original position (~407 nm), and the addition of Al^{3+} ions with 30 μM concentration showed luminescence turn-on (2.1 times increased) behavior along with the blue shifting. This result indicates slight reduction (~5%) in luminescence enhancement. As a result, **1** shows reasonable recyclability and reproducibility of luminescence after regeneration.

To explain the observed luminescence titration behaviors in the presence of these metal ions, we considered two important factors: (i) Differential types of interactions of the free nitrogen atom (NH) of the traizole with the metal ions and (ii) Lewis acid−base interactions between the metal ions and the free amino groups of DATZ of the MOF. Among these ions, charge-to-size ratio of Al^{3+} ions is so high that it is expected to cause rupture of the N−H bonds of the triazole ring to form triazolate and hydronium ions (H_3O^+) in aqueous medium,[27] whereas the free amino groups of DATZ act as simple electron donor to Al^{3+} ions through Lewis acid−base type interactions.

DOI: 10.1021/acs.inorgchem.5b00688
Inorg. Chem. 2015, 54, 6373−6379

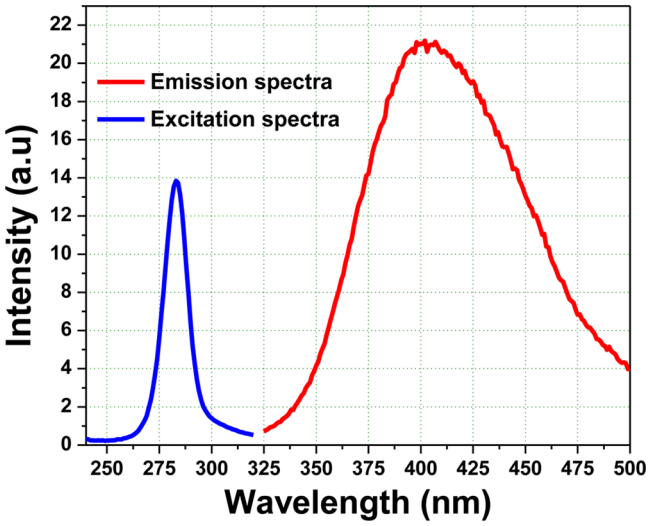

Figure 2. Excitation spectra (monitored at λ_{em} = 407 nm) and emission spectra (monitored at λ_{ex} = 283 nm) of **1** dispersed in water.

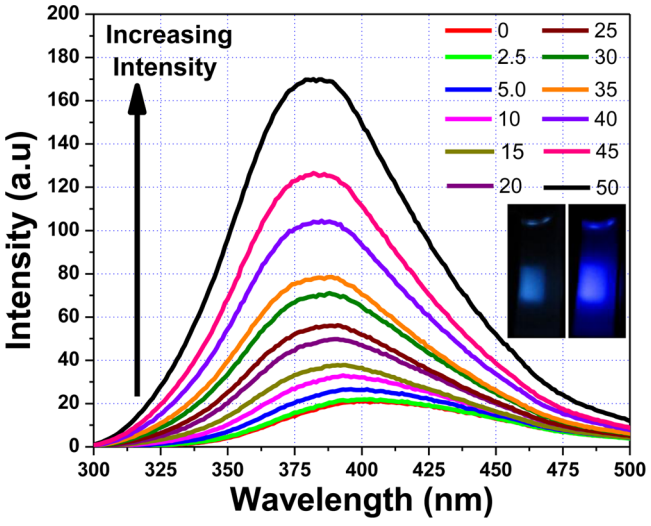

Figure 3. (a) Emission spectra of **1** dispersed in water upon incremental addition of water solution of Al^{3+} ions (λ_{ex} = 283 nm). Final concentration of Al^{3+} ions in the medium is indicated in the legend in micromolar unit. Note the blue shifting with the incremental addition of Al^{3+} ions. (inset) Photographs showing the original luminescence of **1** in water and the enhanced one in the presence of 50 μM of Al^{3+} ions.

It is likely that the possibility of strong electrostatic interactions between the Al^{3+} ions and triazolates (anionic) is responsible for the blue shifting of the emission peak with the incremental addition of the Al^{3+} ions. Additionally, the formation of triazolate increases the overall electron density on DATZ, which resulted in turn-on luminescence behavior. However, in the case of all other metal ions, both free nitrogen (NH) of triazole ring and the amino groups act as Lewis base. It is likely the reduced electron density on the traizole ring through Lewis acid−base interactions is responsible for luminescence quenching. The schematic of the above interactions of the Al^{3+} ions and the other metal ions with the DATZ ligand are shown in Figure 6.

To prove the above mechanism of the luminescence turn-on behavior for Al^{3+} ions, we performed the titrations in acidic aqueous medium where the possibility of the formation of

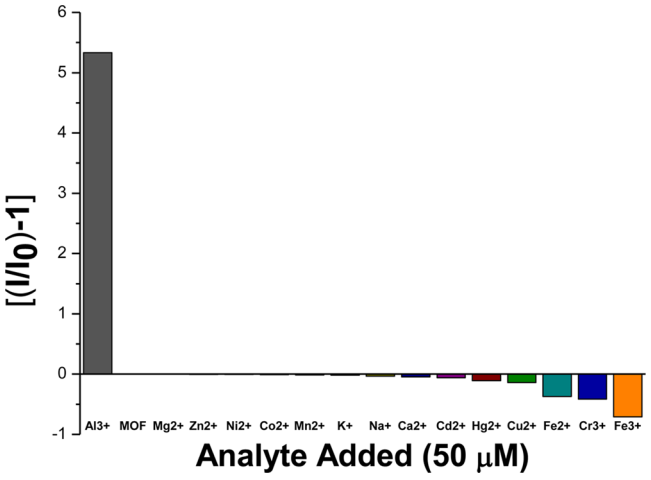

Figure 4. Changes of luminescence intensity with respect of emission of **1** (at 407 nm) with 50 μM of different metal ions.

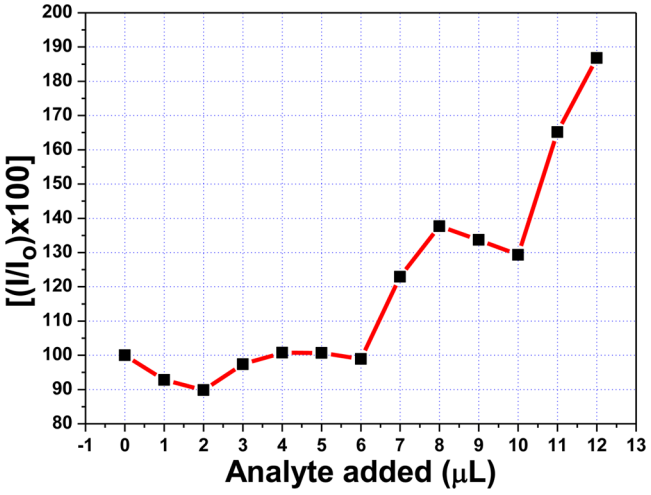

Figure 5. Changes in percentage of luminescence intensity of **1** (at 407 nm) upon the addition of water solution of Fe^{3+} ions followed by Al^{3+} ions.

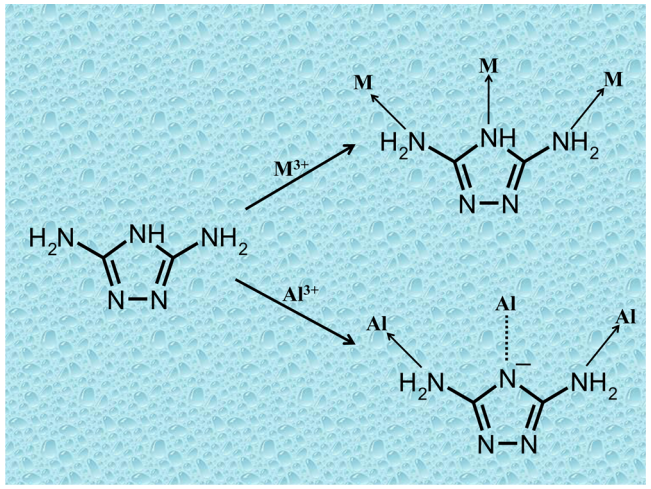

Figure 6. Schematic of differential types of interactions of Al^{3+} ions and all other metal ions (M^{3+}) with the DATZ ligand unit of **1**. The Lewis acid−based interactions are represented using the arrows, and the electrostatic interactions (only for Al^{3+} ions) are represented using dotted line.

DOI: 10.1021/acs.inorgchem.5b00688
Inorg. Chem. 2015, 54, 6373−6379

anionic triazolate is expected to reduce. For this purpose 20 μL of 0.01 M aqueous solution of HCl solution was added to the aqueous mixture of the MOF prior to the luminescence titration using Al^{3+} ions. The results show 2.08 times enhancement in luminescence intensity upon the addition of 50 μM Al^{3+} ions, which is nearly 3 times less than the value obtained in original pure aqueous medium (see Supporting Information, Figure S28). The lesser amount of turn-on behavior strongly supports the interaction between the Al^{3+} ions and MOF through the triazolate ring.

CONCLUSION

In conclusion, a two-dimensional MOF with free functional sites have been synthesized. The compound demonstrates highly sensitive sensing of Al^{3+} ions in aqueous medium through luminescence enhancement (turn-on) along with the blue shifting of the emission wavelength. In contrast to this, in the presence of other common metal ions the compound shows simple luminescence quenching. The luminescence turn-on behavior for Al^{3+} in the presence of quenchable metal ions makes this MOF a selective Al^{3+} sensor in aqueous medium. Detailed experimental studies explained differential types of interactions between Al^{3+} ions and all other common metal ions are important factors for observed luminescence behaviors. The present work, for the first time, demonstrates the potential for the use of MOF for the sensing of Al^{3+} in aqueous medium. More importantly, the observed detection limit of 57.5 ppb, which is considerably lower than the higher limit of U.S. EPA recommendation of Al^{3+} ion for drinking water (200 ppb), make this MOF a useful Al^{3+} sensor for real-life application.

ASSOCIATED CONTENT

Supporting Information

Tabulated IR data and selected bond angles, IR spectrum, emission spectra, PXRD pattern, TGA curve, DSC curve, ORTEP and other illustrations of complexes and portions of complexes, SEM image, luminescence-based titration plots, plots of molar magnetic susceptibility versus temperature, and crystallographic data (CIF). The Supporting Information is available free of charge on the ACS Publications website at DOI: 10.1021/acs.inorgchem.5b00688. CCDC: 1050854 contain the crystallographic data for this paper. These data can be obtained free of charge from The Cambridge Crystallographic Data Center (CCDC) via www.ccdc.cam.ac.uk/data_request/cif.

AUTHOR INFORMATION

Corresponding Author

*E-mail: partha.mahata@bose.res.in or parthachem@gmail.com.

Notes

The authors declare no competing financial interest.

ACKNOWLEDGMENTS

This work was supported by INSPIRE faculty research grant (No. IFA12-CH-69) and fast track project grant (No. SB/FT/CS114/2012) of Department of Science and Technology, Government of India. P.M. also thanks Dr. S. Mandal, IISER, Thiruvananthapuram, and his research group for their support to execute the project, especially for SCXRD data.

REFERENCES

(1) (a) Leddy, J. J. In *Electrochemistry, Past and Present;* Stock, J. T., Orna, M. V., Eds.; ACS Symposium Series; American Chemical Society: Washington, DC, 1989; Chapter 33, Vol. *390*, p 478. (b) Harber, F. *J. Ind. Eng. Chem.* **1914**, *6*, 325. (c) Strickland, D. M. *Ind. Eng. Chem.* **1923**, *15*, 566. (d) Nelson, P. G. *J. Chem. Educ.* **1991**, *68*, 732.

(2) (a) Ding, W. H.; Cao, W.; Zheng, X.-J.; Fang, D.-C.; Wong, W.-T.; Jin, L.-P. *Inorg. Chem.* **2013**, *52*, 7320. (b) Burwen, D. R.; Olsen, S. M.; Bland, L. A.; Arduino, M. J.; Reid, M. H.; Jarvis, W. R. *Kidney Int.* **1995**, *48*, 469. (c) Berthon, G. *Coord. Chem. Rev.* **2002**, *228*, 319. (d) Yousef, M. I.; EI-Morsy, A. M. A.; Hassan, M. S. *Toxicology* **2005**, *215*, 97. (e) Bielarczyk, H.; Jankowska, A.; Madziar, B.; Matecki, A.; Michno, A.; Szutowich, A. *Neurochem. Int.* **2003**, *42*, 323.

(3) (a) Barcelo', J.; Poschenrieder, C. *Environ. Exp. Bot.* **2002**, *48*, 75. (b) Valeur, B.; Leray, I. *Coord. Chem. Rev.* **2000**, *205*, 3. (c) Rogers, M. A. M.; Simon, D. G. *Age Ageing* **1999**, *28*, 205. (d) Krejpcio, Z.; Wojciak, R. W. *Pol. J. Environ. Stud.* **2002**, *11*, 251.

(4) (a) Nayak, P. *Environ. Res.* **2002**, *89*, 101. (b) Vallejos, S.; Muñoz, A.; Ibeas, S.; Serna, F.; García, F. C.; García, J. M. *ACS Appl. Mater. Interfaces* **2015**, *7*, 921.

(5) Fasman, G. D. *Coord. Chem. Rev.* **1996**, *149*, 125.

(6) (a) Keep, K. P. *Chem. Rev.* **2012**, *112*, 5193. (b) Perl, D. P.; Brody, A. R. *Science* **1980**, *208*, 297. (c) Shokrollahi, A.; Ghaedi, M.; Niband, M. S.; Rajabi, H. R. *J. Hazard. Mater.* **2008**, *151*, 642. (c) Salifoglou, A. *Coord. Chem. Rev.* **2002**, *228*, 297. (d) Samanta, S.; Goswami, S.; Hoque, Md. N.; Ramesh, A.; Das, G. *Chem. Commun.* **2014**, *50*, 11833.

(7) (a) Lakowicz, J. R. *Principles of Fluorescence Spectroscopy,* 3rd ed.; Kluwer Academic: New York, 2006. (b) Shustova, N. B.; Cozzolino, A. F.; Reineke, S.; Baldo, M.; Dincă, M. *J. Am. Chem. Soc.* **2013**, *135*, 13326.

(8) (a) Park, H. M.; Oh, B. N.; Kim, J. H.; Qiong, W.; Hwang, I. H.; Jung, K.-D.; Kim, C.; Kim, J. *Tetrahedron Lett.* **2011**, *52*, 5581. (b) Kim, S. H.; Choi, H. S.; Kim, J.; Joong, S.; Quang, D. T.; Kim, J. S. *Org. Lett.* **2010**, *12*, 560. (c) Maity, D.; Govindaraju, T. *Chem. Commun.* **2010**, *46*, 4499. (d) Lee, J.; Kim, H.; Kim, S.; Noh, J. Y.; Song, E. J.; Kim, C.; Kim, J. *Dyes Pigm.* **2013**, *96*, 590. (e) Cheng, X.-Y.; Wang, M.-F.; Yang, Z.-Y.; Li, Y.; Li, T.-R.; Liu, C.-J.; Zhou, Q.-X. *J. Coord. Chem.* **2013**, *66*, 1847. (f) Liao, Z.-C.; Yang, Z.-Y.; Li, Y.; Wang, B.-D.; Zhou, Q.-X. *Dyes Pigm.* **2013**, *97*, 124. (g) Wang, Y.-W.; Yu, M.-X.; Yu, Y.-H.; Bai, Z.-P.; Shen, Z.; Li, F.-Y.; You, X.-Z. *Tetrahedron Lett.* **2009**, *50*, 6169. (h) Maity, S. B.; Bharadwaj, P. K. *Inorg. Chem.* **2013**, *52*, 1161. (i) Ma, T.-H.; Dong, M.; Dong, Y.-M.; Wang, Y.-W.; Peng, Y. A. *Chem.—Eur. J.* **2010**, *16*, 10313. (j) Tiwari, K.; Mishra, M.; Singh, V. P. *RSC Adv.* **2013**, *3*, 12124. (k) Jiang, C.; Tang, B.; Wang, C.; Zhang, X. *Analyst* **1996**, *121*, 317. (l) Jiang, C.; Tang, B.; Wang, R.; Yen, J. *Talanta* **1997**, *44*, 197. (m) Mánuel-Vez, M. P.; Garcia-Vargas, M. *Talanta* **1994**, *41*, 1553.

(9) (a) Suryawanshi, V. D.; Gore, A. H.; Dongare, P. R.; Anbhule, P. V.; Patil, S. R.; Kolekar, G. B. *Spectrochim. Acta, Part A* **2013**, *114*, 681. (b) Guo, Y.-Y.; Yang, L.-Z.; Ru, J.-X.; Yao, X.; Wu, J.; Dou, W.; Qin, W.-W.; Zhang, G.-L.; Tang, X.-L.; Liu, W.-S. *Dyes Pigm.* **2013**, *99*, 693. (c) Vallejos, S.; Muñoz, A.; Ibeas, S.; Serna, F.; García, F. C.; García, J. M. *J. Hazard. Mater.* **2014**, *276*, 52.

(10) (a) Li, M.; Li, D.; O'Keeffe, M.; Yaghi, O. M. *Chem. Rev.* **2014**, *114*, 1343. (b) Mahata, P.; Natarajan, S. *Chem. Soc. Rev.* **2009**, *38*, 2304.

(11) (a) Suh, M. P.; Park, H. J.; Prasad, T. K.; Lim, D.-W. *Chem. Rev.* **2012**, *112*, 782. (b) Zhou, H. C.; Long, J. R.; Yaghi, O. M. *Chem. Rev.* **2012**, *112*, 673.

(12) (a) Wu, H.; Gong, Q.; Olson, D. H.; Li, J. *Chem. Rev.* **2012**, *112*, 836. (b) Sumida, K.; Rogow, D. L.; Mason, J. A.; McDonald, T. M.; Bloch, E. D.; Herm, Z. R.; Bae, T.-H.; Long, J. R. *Chem. Rev.* **2012**, *112*, 724. (c) Li, J.-R.; Sculley, J.; Zhou, H.-C. *Chem. Rev.* **2012**, *112*, 869.

(13) (a) Yoon, M.; Srirambalaji, R.; Kim, K. *Chem. Rev.* **2012**, *112*, 1196. (b) Kozachuk, O.; Luz, L.; Xamena, F. X. L.; Noei, H.; Kauer, M.; Albada, H. B.; Bloch, E. D.; Marler, B.; Wang, Y. M.; Muhler, M.;

DOI: 10.1021/acs.inorgchem.5b00688
Inorg. Chem. 2015, 54, 6373−6379

Fischer, R. A. *Angew. Chem., Int. Ed.* **2014**, *53*, 7058. (c) Ma, L.; Abney, C.; Lin, W. *Chem. Soc. Rev.* **2009**, *38*, 1248. (d) Moon, H. R.; Lim, D.-W.; Suh, M. P. *Chem. Soc. Rev.* **2013**, *42*, 1807.
(14) (a) Kurmoo, M. *Chem. Soc. Rev.* **2009**, *38*, 1353. (b) Mahata, P.; Natarajan, S.; Panissod, P.; Drillon, M. *J. Am. Chem. Soc.* **2009**, *131*, 10140.
(15) (a) Della Rocca, J.; Liu, D.; Lin, W. *Acc. Chem. Res.* **2011**, *44*, 957. (b) Horcajada, P.; Gref, R.; Baati, T.; Allan, P. K.; Maurin, G.; Couvreur, P.; Férey, G.; Morris, R. E.; Serre, C. *Chem. Rev.* **2012**, *112*, 1232.
(16) (a) Wu, P.; Wang, J.; He, C.; Zhang, X.; Wang, Y.; Liu, T.; Duan, C. *Adv. Funct. Mater.* **2012**, *22*, 1698. (b) Liu, D.; Lu, K.; Poon, C.; Lin, W. *Inorg. Chem.* **2014**, *53*, 1916.
(17) (a) Horike, S.; Umeyama, D.; Kitagawa, S. *Acc. Chem. Res.* **2013**, *46*, 2376. (b) Yoon, M.; Suh, K.; Natarajan, S.; Kim, K. *Angew. Chem., Int. Ed.* **2013**, *52*, 2688. (c) Zhao, X.; Mao, C.; Bu, X.; Feng, P. *Chem. Mater.* **2014**, *26*, 2492.
(18) (a) Wanderley, M. M.; Wang, C.; Wu, C.-D.; Lin, W. *J. Am. Chem. Soc.* **2012**, *134*, 9050. (b) Shustova, N. B.; Cozzolino, A. F.; Reineke, S.; Baldo, M.; Dincă, M. *J. Am. Chem. Soc.* **2013**, *135*, 13326. (c) Lu, Z.-Z.; Zhang, R.; Li, Y.-Z.; Guo, Z.-J.; Zheng, H.-G. *J. Am. Chem. Soc.* **2011**, *133*, 4172. (d) Guo, Y.; Feng, X.; Han, T.; Wang, S.; Lin, Z.; Dong, Y.; Wang, B. *J. Am. Chem. Soc.* **2014**, *136*, 15485−15488.
(19) (a) Jayaramulu, K.; Narayanan, R. P.; George, S. J.; Maji, T. K. *Inorg. Chem.* **2012**, *51*, 10089. (b) Yang, C.-X.; Ren, H.-B.; Yan, X.-P. *Anal. Chem.* **2013**, *85*, 7441. (c) Qin, J.-S.; Zhang, S.-R.; Du, D.-Y.; Shen, P.; Bao, S.-J.; Lan, Y.-Q.; Su, Z.-M. *Chem.—Eur. J.* **2014**, *20*, 5625. (d) Han, Z.-B.; Xiao, Z.-Z.; Hao, M.; Yuan, D.-Q.; Liu, L.; Wei, N.; Yao, H.-M.; Zhou, M. *Cryst. Growth Des.* **2015**, *15*, 531. (e) Cao, J.; Gao, Y.; Wang, Y.; Du, C.; Liu, Z. *Chem. Commun.* **2013**, *49*, 6897. (f) Bhattacharyya, S.; Chakraborty, A.; Jayaramulu, K.; Hazra, A.; Maji, T. K. *Chem. Commun.* **2014**, *50*, 13567. (g) Xiang, Z.; Fang, C.; Leng, S.; Cao, D. *J. Mater. Chem. A* **2014**, *2*, 7662. (h) Hao, J.-N.; Yan, B. *J. Mater. Chem. C* **2014**, *2*, 6758. (i) Zheng, M.; Tan, H.; Xie, Z.; Zhang, L.; Jing, X.; Sun, Z. *ACS Appl. Mater. Interfaces* **2013**, *5*, 1078. (j) Xu, X.-Y.; Yan, B. *ACS Appl. Mater. Interfaces* **2015**, *7*, 721. (k) Tang, Q.; Liu, S.; Liu, Y.; Miao, J.; Li, S.; Zhang, L.; Shi, Z.; Zheng, Z. *Inorg. Chem.* **2013**, *52*, 2799. (l) Chen, Z.; Sun, Y.; Zhang, L.; Sun, D.; Liu, F.; Meng, Q.; Wang, R.; Sun, D. *Chem. Commun.* **2013**, *49*, 11557. (m) Zhou, J.-M.; Shi, W.; Li, H.-M.; Li, H.; Cheng, P. *J. Phys. Chem. C* **2014**, *118*, 416. (n) Chen, B.; Wang, L.; Xiao, Y.; Fronczek, F. R.; Xue, M.; Cui, Y.; Qian, G. *Angew. Chem., Int. Ed.* **2009**, *48*, 500.
(20) (a) Pramanik, S.; Zheng, C.; Zhang, X.; Emge, T. J.; Li, J. *J. Am. Chem. Soc.* **2011**, *133*, 4153. (b) Hu, Z.; Deibert, B. J.; Li, J. *Chem. Soc. Rev.* **2014**, *43*, 5815. (c) Kim, T. K.; Lee, J. H.; Moon, D.; Moon, H. R. *Inorg. Chem.* **2013**, *52*, 589. (d) Singha, D. K.; Bhattacharya, S.; Majee, P.; Mondal, S. K.; Kumar, M.; Mahata, P. *J. Mater. Chem. A* **2014**, *2*, 20908.
(21) Rocha, J.; Carlos, L. D.; Paz, F. A. A.; Ananias, D. *Chem. Soc. Rev.* **2011**, *40*, 926.
(22) *SMART (V 5.628), SAINT (V 6.45a), XPREP, SHELXTL;* Bruker AXS Inc.: Madison, WI, 2004.
(23) Sheldrick, G. M. *Siemens area correction absorption correction program;* University of Göttingen: Göttingen, Germany, 1994.
(24) Sheldrick, G. M. *SHELXL-97 program for crystal structure solution and refinement;* University of Göttingen: Göttingen, Germany, 1997.
(25) Farrugia, J. L. *J. Appl. Crystallogr.* **1999**, *32*, 837.
(26) National Secondary Drinking Water Regulations of the US EPA: Maximum Contaminant Levels, http://water.epa.gov/drink/contaminants/secondarystandards.cfm, accessed 24 March 2013.
(27) Huheey, J.; Keiter, E. A.; Keiter, R. L. *Inorganic Chemistry: Principles of Structure and Reactivity,* 4th ed.; Pearson Education: New York, 2000.

DOI: 10.1021/acs.inorgchem.5b00688
Inorg. Chem. 2015, 54, 6373−6379